

Research Article

Single-Layer Planar Monopole Antenna-Based Artificial Magnetic Conductor (AMC)

Ali Abdulateef Abdulbari ^{1,2}, Sharul Kamal Abdul Rahim ^{1,2}, Firas Abedi ³,
Ping Jack Soh ⁴, Ali Hashim ⁵, Rami Qays ⁶,
Sarosh Ahmad ⁷, and Mohammed Yousif Zeain⁸

¹Wireless Communication Centre (WCC), School of Electrical Engineering, Universiti Teknologi Malaysia (UTM), Skudai 81310, Malaysia

²Department of Computer Techniques Engineering, Imam Al-Kadhum College (IKC), Thi-Qar, Baghdad, Iraq

³Department of Mathematics, College of Education, Al-Zahraa University for Women Karbala, Karbala, Iraq

⁴Centre for Wireless Communications (CWC), University of Oulu, P. O Box 4500, 90014 Oulu, Finland

⁵Department of Computer Technical Engineering, College of Information Technology, Imam Ja'afar Al-Sadiq University, 66002 Al-Muthanna, Iraq

⁶Department of Medical Instrumentation Techniques Engineering, Al-Mustaqbal University College, Hillah 51001, Iraq

⁷Department of Signal Theory and Communications, Universidad Carlos III de Madrid, Leganes 28911, Madrid, Spain

⁸Centre for Telecommunication Research and Innovation (CeTRI), Faculty of Electronics and Computer Engineering, Universiti Teknikal Malaysia Melaka (UTeM), Melaka, Malaysia

Correspondence should be addressed to Ali Abdulateef Abdulbari; alilateefutm@gmail.com

Received 21 February 2022; Revised 13 May 2022; Accepted 31 May 2022; Published 21 July 2022

Academic Editor: Paolo Baccarelli

Copyright © 2022 Ali Abdulateef Abdulbari et al. This is an open access article distributed under the Creative Commons Attribution License, which permits unrestricted use, distribution, and reproduction in any medium, provided the original work is properly cited.

In this paper, a coplanar waveguide (CPW)-fed patch antenna is fabricated on a layer of metasurface to increase gain. The antenna is fabrication on Roger substrate with a thickness of 0.25 mm, with the overall dimension of the proposed design being $45 \times 30 \times 0.25 \text{ mm}^3$. The size of the patch antenna is $24 \times 14 \times 0.25 \text{ mm}^3$, and the AMC unit cell is $22 \times 22 \times 0.25 \text{ mm}^3$. This metasurface is designed based on the split-ring resonator unit cells forming an array of the artificial magnetic conductor (AMC). Meanwhile, the antenna operation on 3.5 GHz is enabled by etching a split-ring resonator slot on the ground plane with a small gap to enhance antenna gain and improve impedance bandwidth when integrated with a metasurface. This simulation planer monopole antenna is applied for 5G application. The experimenter test is applied for the antenna performance in terms of return loss, gain, and radiation patterns. The operating frequency range with and without MTM is from 3.41 to 3.68 GHz (270 MHz) and 3.37 to 3.55 GHz (180 MHz), respectively, with gain improvements of about 2.7 dB (without MTM) to 6.0 dB (with MTM) at 3.5 GHz. The maximum improvement of the gain is about 42% when integrated with the AMC. The AMC has solved several issues to overcome the typical limitation in conventional antenna design. A circuit model is also proposed to simplify the estimation of the performance of this antenna at the desired frequency band. The proposed design is simulated by CST microwave studio. Finally, the antenna is fabricated and measured. Result comparison between simulations and measurements indicates a good agreement between them.

1. Introduction

In recent years, mobile communication systems are challenged by the increasing number of connected devices and higher data rates, low latency, cost, and energy usage.

The expected inclusion of Internet of things (IoT) devices totaling more than 20 billion units [1, 2] will require speeds of more than 10 Gbps. The fifth-generation (5G) services have been introduced, with new strategies to optimize the limited spectrum to achieve such data rates

[3, 4]. In many countries, the 5G new radio frequency band has been standardized below 6 GHz. 78 GHz frequency is a particular band in the range from 3.3 to 3.8 GHz which has been adapted 3 GHz spectrum congestion cellular networks [6].

Planar antennas have received research attention in recent decades due to their attractive benefits—low cost, low profile, ease of integration with other circuits, and suitability for multipolarization antennas [7, 8]. In recent years, these antennas have been investigated to ensure size reduction, enhanced bandwidth, and improved efficiency [9, 10]. Different antennas have been proposed to achieve miniaturization and bandwidth improvements such as circular [11, 12], elliptical [13], triangular [14], fractal [15], E-shaped [16], and U-shaped antennas [17]. While it is ideal to use multiband antennas with wide operating bands, the use of asymmetric parasitic elements will result in radiation pattern variations with frequency. On the other hand, adding slots in the radiating patch is a very effective method to increase the bandwidth without increasing the antenna size. However, this technique is mainly suitable for thicker substrates [18, 19]. Besides that, other techniques such as modification of the ground structure or stacking of multiple substrate layers potentially improve the gain of patch antennas [20]. For the former, several examples include the use of a U-shaped slot, L-shaped arm, or interlocking semielliptical holes in the ground plane, or feeding a rectangular and hexagonal patch using the coplanar waveguide (CPW) technique [21, 22].

Metamaterials (MTM) are artificial magnetic materials that do not exist in nature, but their properties can be emulated by special arrangements of existing materials [23]. Meanwhile, using technology MTM in the design of antenna structure may be caused obtain a small size will use this antenna for the large frequency bandwidth [24]. It is increasingly popular to be used to improve the antenna performance by increasing the directivity and gain and reducing the back radiation of patch antennas [25, 26]. One of the types of metamaterials widely used in antennas is the electromagnetic band gap (EBG) and artificial magnetic conductors [27]. To enhance gain, EBG or artificial magnetic conductor (AMC) layers can be integrated with antennas with a small distance between them [28], which maintains the antenna's overall low profile. The novelty of the proposed antenna is in terms of its compact size with metamaterial, high gain of the antenna, and improved bandwidth. In this work, the design of a planar monopole antenna with AMC is proposed for compact size and high gain enhancement. It operates in the 3.5 GHz band for 5G applications. The contribution of the AMC plane is evaluated by comparing the performance of the antenna with and without the AMC reflector. It is observed that the AMC-backed antenna increased its gain by more than 3 dB at 3.5 GHz. The next section will explain the design of the patch antenna and the AMC unit cell, followed by the presentation of the circuit model, results, and discussion. Finally, Section 5 concludes this paper with a summary of the findings.

2. Antenna Design

This section discusses the design methodology of the planar monopole antenna using discrete ground circular rings. In order to verify the scattering parameters of this proposed antenna, the equivalent circuit model is also made for the validity of the 50-ohm input impedance and S_{11} .

2.1. Antenna Design Procedure. The structure of the proposed design is printed on Rogers Duroid RT5880LZ substrate with the relative permittivity of $\epsilon_r = 2$, loss tangent of $\tan\delta = 0.0021$, and the standard thickness of 0.25 mm. The overall dimension of the antenna is $45 \times 30 \times 0.25 \text{ mm}^3$. The radiating patch is fed by a single 50 Ω microstrip feed line connected to the antenna. The top view of the proposed antenna and defected ground structure (DGS) are presented in Figure 1. Figure 2 illustrates the step of the parametric study of the proposed antenna. The optimized parameters of the planar monopole antenna with the defected ground structure are listed in Table 1. In the first step, a simple patch is designed. Then, in the next step, slots are added on the right side of the radiating patch and truncated from its edge to resonate at 3.8 GHz. The gain will then be improved when discrete ground circular rings are added to the structure [29]. To calculate the initial antenna and feed line sizes, the procedure outlined in [30] is used as a start.

3. Design of the AMC Unit Cell

3.1. AMC-Unit Cell. The structure of the proposed AMC-unit cell is presented in Figure 3(a). It is designed on Rogers RT5880LZ substrate with the thickness of 0.25 mm, dielectric permittivity of 2, and loss tangent of 0.002, $\epsilon_r = 2$, loss tangent of $\tan\delta = 0.0021$. The dimensions of the ring unit cell radius are $R_1 = 4.90 \text{ mm}$, $R_2 = 7.94 \text{ mm}$, $R_3 = 10.95 \text{ mm}$, $R_4 = 13.96 \text{ mm}$, whereas the split gap (G) is 1 mm and ring width (W) is 0.5 mm. The overall size of the square-shaped unit cell is $22 \times 22 \times 0.25 \text{ mm}^3$. The comparison of the reflection phase of a square patch unit cell with and without the SRR is presented in Figure 3(b).

3.2. Design of the AMC-Backed Antenna. Two units of the proposed unit cell are spaced at a 1 mm distance from each other to form the AMC plane. The length and width of the AMC plane, " L_m " and " W_m ", are 44 mm and 22 mm, respectively. It is integrated onto the reverse side of the antenna to operate as a reflector. This is aimed at reducing coupling, maintaining a compact size, and improving the antenna's forward gain. The AMC plane is integrated at a distance $D = 15 \text{ mm}$ from the radiator, as shown in Figure 4(a). To study the effects of the AMC plane on the performance of the antenna, the S_{11} of the proposed AMC-backed design is simulated and presented in Figure 4(b). It is seen that the reflection coefficient of the antenna improves by increasing the distance D from the AMC plane.

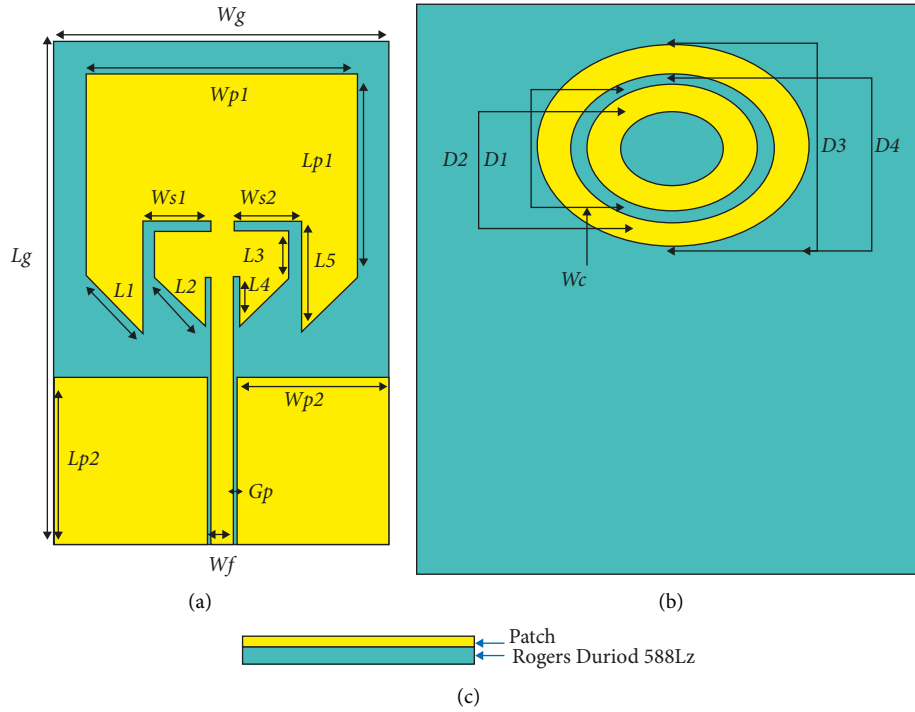


FIGURE 1: (a) Top view of the proposed patch antenna. (b) Back view of the antenna. (c) Side view of the patch antenna.

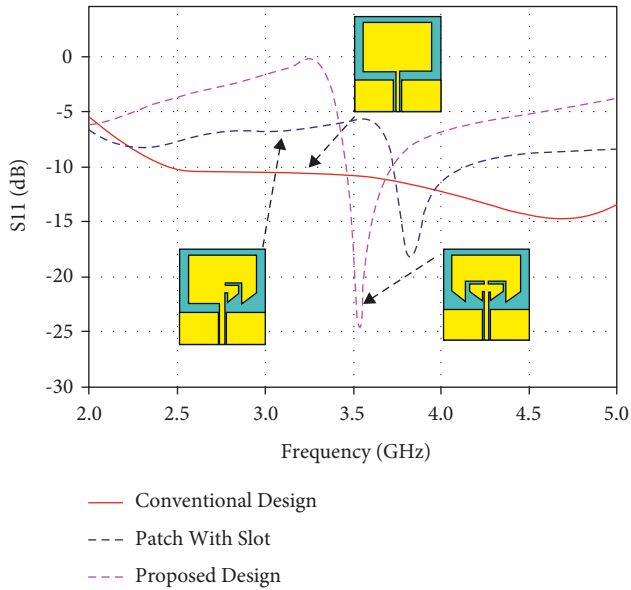


FIGURE 2: Reflection coefficients of the patch antenna in different design steps.

4. Equivalent Circuit Model

An equivalent circuit model of the patch antenna and split ring resonator (SRR) is introduced in this section to simplify the estimation of the antenna's resonant frequency, as shown in Figure 5(a). The circuit model consists of an RLC (resistor-inductor-capacitor) circuit connected in series with a capacitor and a resistor [31]. Parameters $L1$ and $C1$ correspond to the inductance and capacitance of the

TABLE 1: Dimensions of the patch antenna.

Parameter	Value (mm)
Wg	30
Lg	45
$Wp1$	24
$Wp2$	13.7
$Lp1$	17
$Lp2$	14
Wf	2
$Ws1$	5
$Ws2$	6
$L1$	7
$L2$	6.36
$L3$	4
$L4$	4.5
$L5$	10
Gp	0.30
Wc	1
$D1$	8
$D2$	10
$D3$	14
$D4$	16

slots and truncated patch, respectively, whereas $C2$ is related to the capacitance between the CPW ground plane and a microstrip line as shown in Figure 5(a). The inductance of the feed line and Z_0 is the characteristic impedance of the line adjusted at $50\ \Omega$. It is noticed that by increasing the values of the capacitor, the reflection coefficient (S_{11}) of the circuit model varies from the higher frequency band to the lower frequency band, and the values of the parameters are given in Table 2. A simple RLC circuit

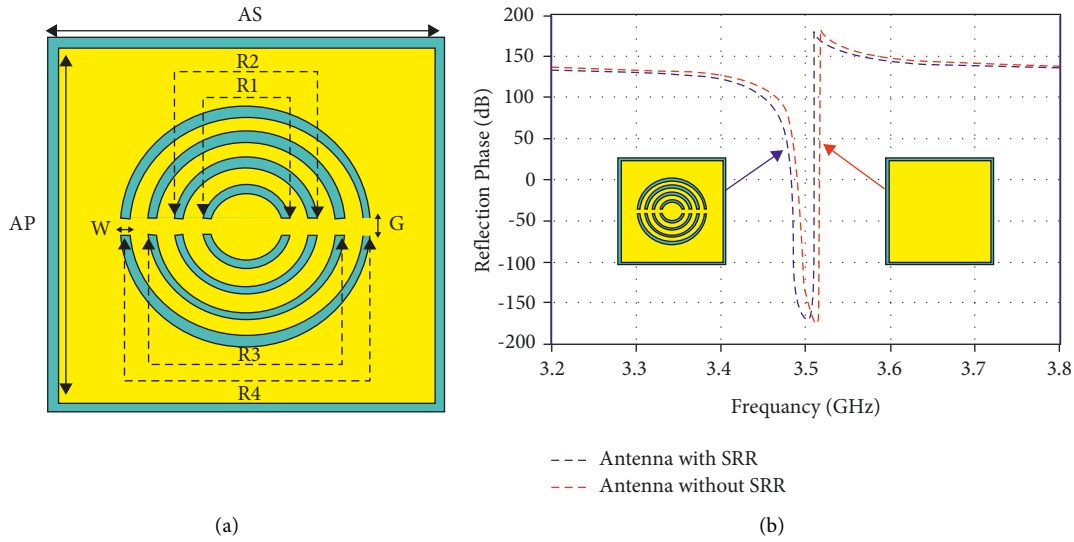


FIGURE 3: (a) Design of the unit cell. (b) Comparison of the AMC-backed antenna with and without SRR.

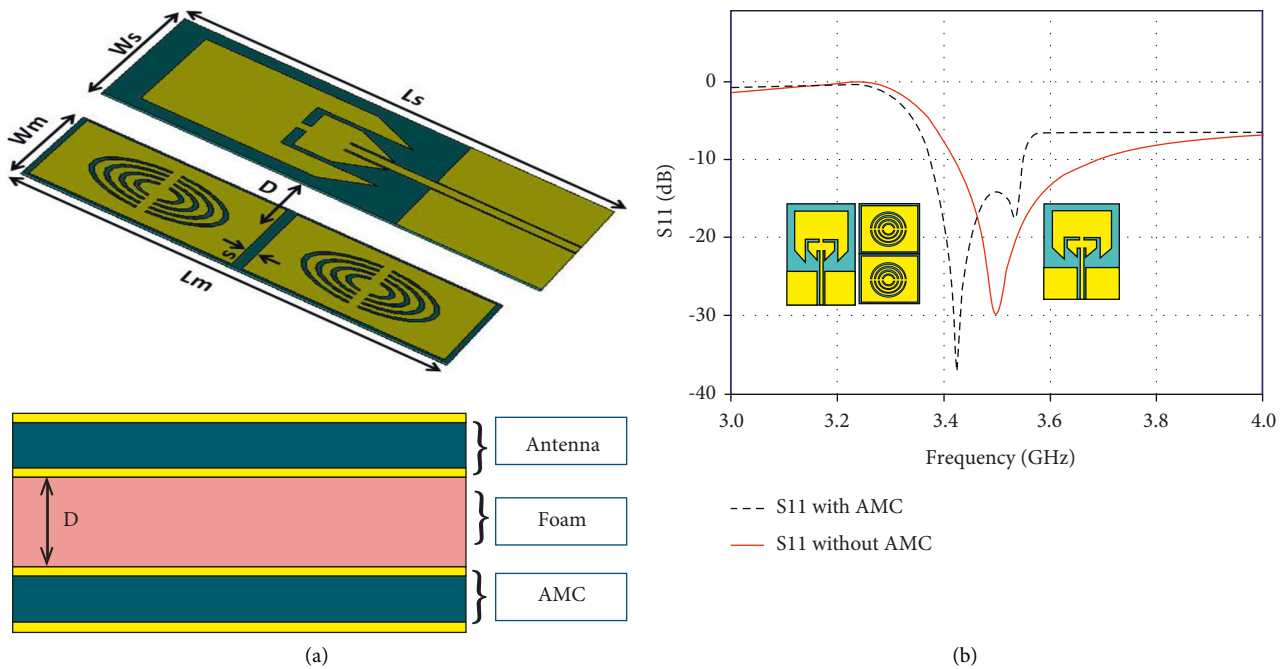


FIGURE 4: (a) Perspective and cross-sectional view of the AMC-backed antenna. (b) $|S_{11}|$ of the antenna with and without AMC plane.

is used to represent the planar monopole antenna while the other resistor and the capacitor are used for the discrete ground circular rings on the reverse side of the antenna substrate. A comparison of S_{11} from the full-wave simulations and the proposed circuit model is presented in Figure 5(b). Estimation of the resonant frequency (f_r) using the equivalent circuit model can be performed using the following equation:

$$f_r = \frac{1}{2\sqrt{L1(C1 + C2)}} \quad (1)$$

5. Results and Discussion

The photograph of the fabricated prototype of the planar monopole antenna with the AMC is illustrated in Figure 6. The reflection coefficient is lower than -10 dB for the desired frequency band antenna both with and without an AMC, with the former having a minimum reflection coefficient of -37.59 dB at 3.49 GHz and the antenna without SRR a reflection coefficient of -29.0 dB at 3.5 GHz. The measured reflection coefficient with and without AMC of -27.0 dB at 3.51 GHz and -34.5 dB at 3.44 GHz is as shown in Figure 7. The gain and bandwidth enhancement capability of the

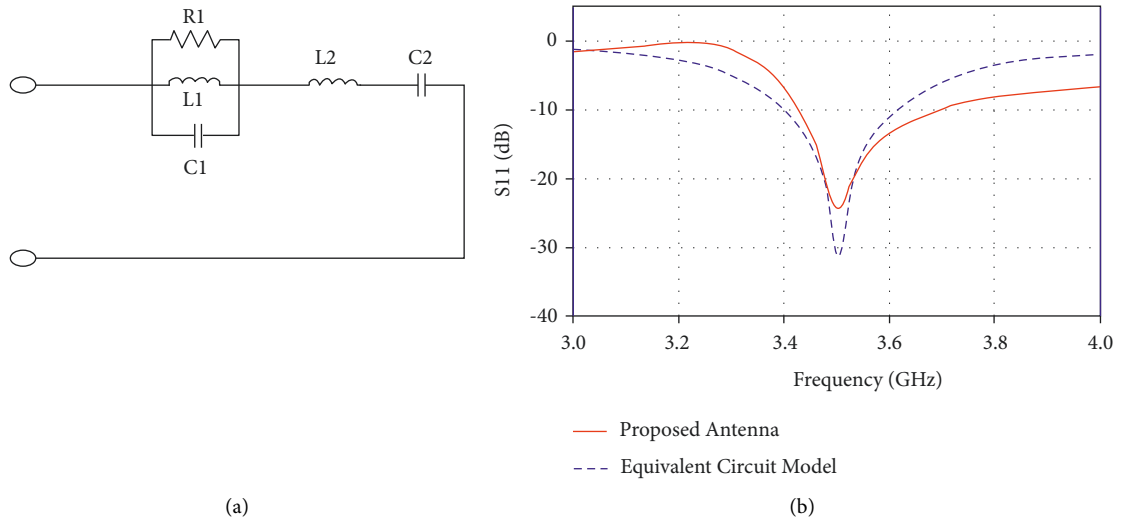


FIGURE 5: (a) Equivalent circuit model of the patch antenna. (b) Comparison of S₁₁ of the antenna from full-wave simulations and the proposed circuit model.

TABLE 2: Values of the components used in the circuit model.

Inductors	Values (nH)	Capacitors	Values (pF)	Resistors	Values (Ω)
L1	0.278	C1	7	R1	70
L2	0.01	C2	1.31	Z ₀	50

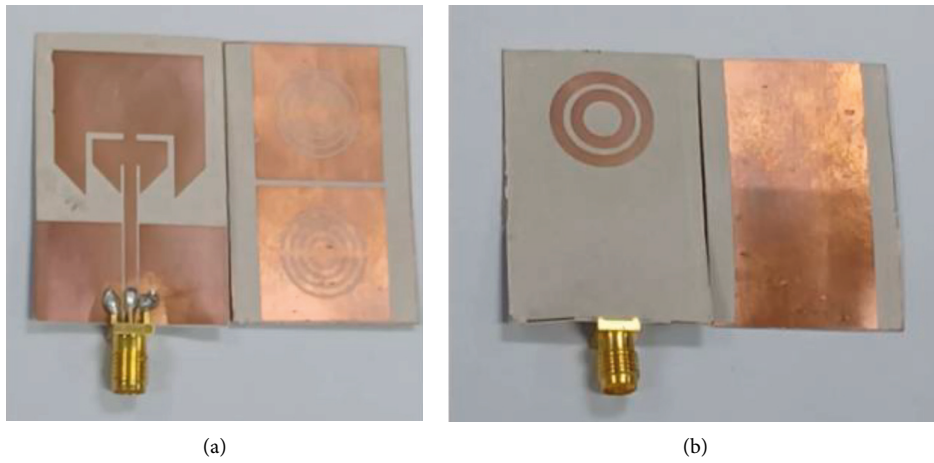


FIGURE 6: Photograph of the fabricated monopole and AMC: (a) front view and (b) back view.

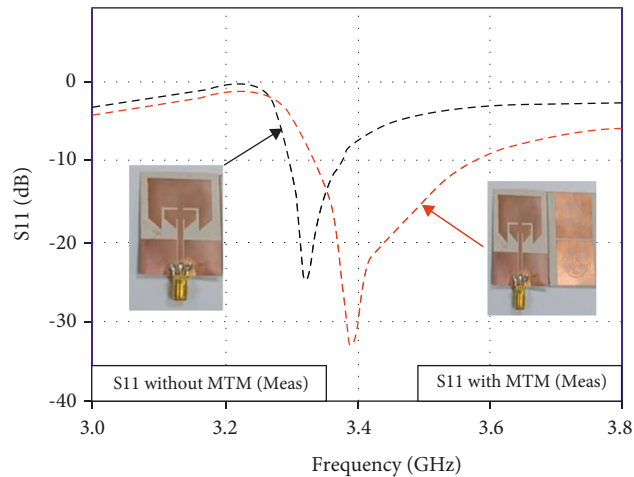


FIGURE 7: Comparison of the measured S₁₁ of the antenna with and without AMC.

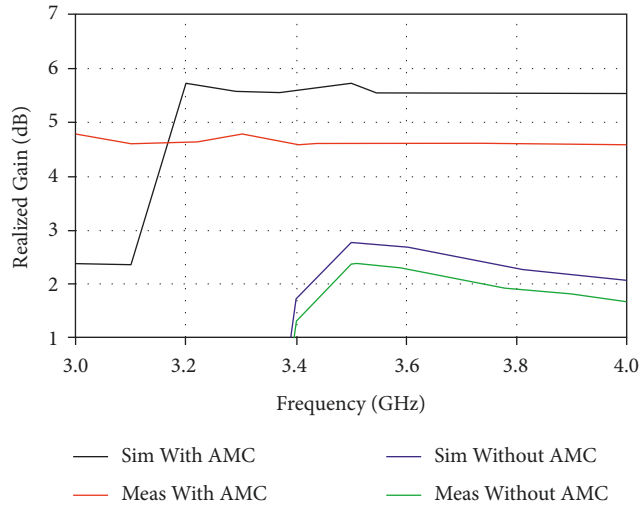


FIGURE 8: Simulated and measured realized gain of the antenna with and without AMC.

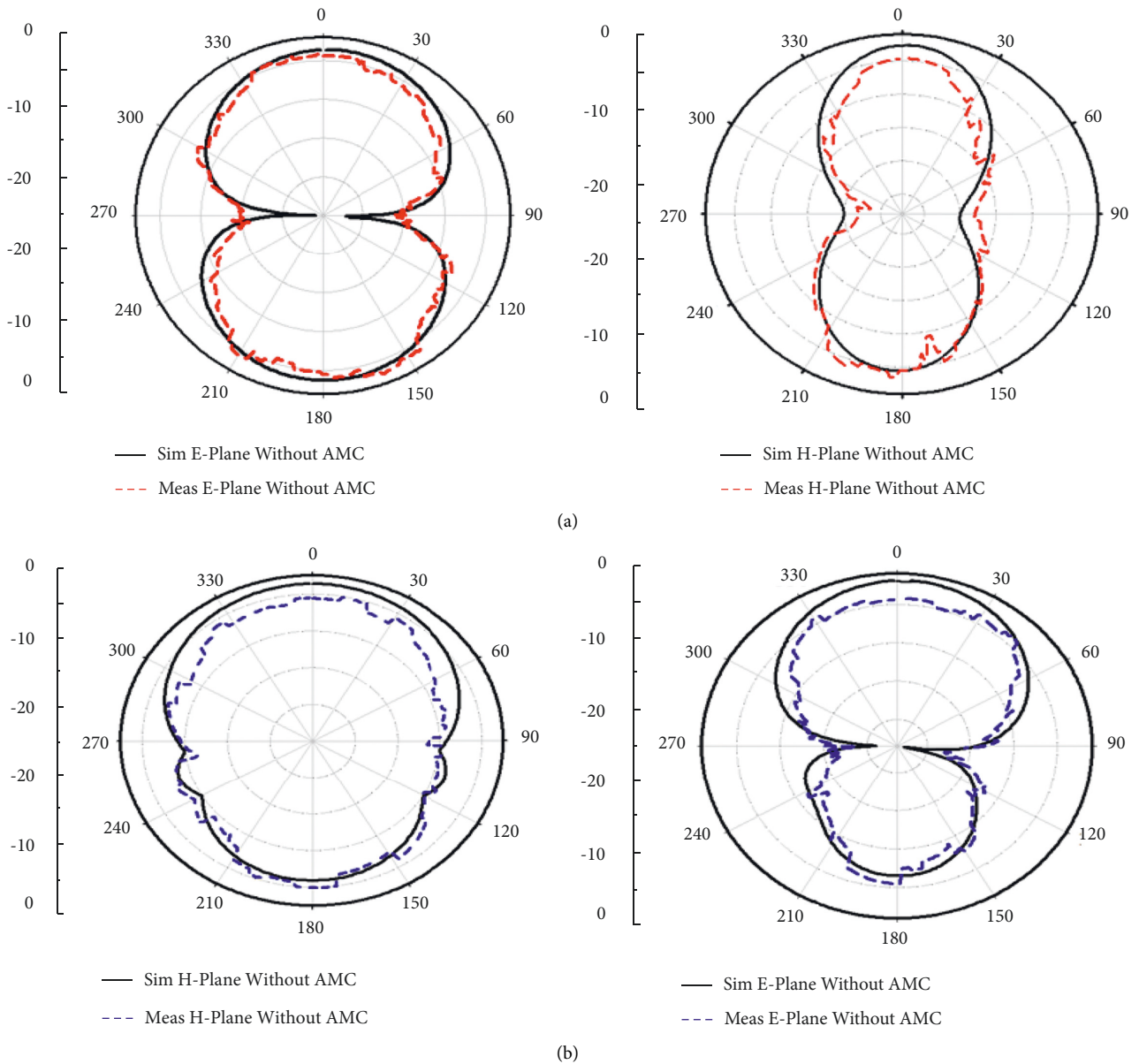


FIGURE 9: Radiation patterns of the proposed antenna: (a) without and (b) with AMC at 3.5 GHz.



FIGURE 10: Measurement setup of the reflection coefficient.

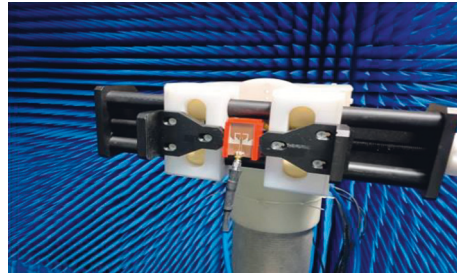


FIGURE 11: Measurement setup of the radiation pattern.

TABLE 3: Comparison between proposed designs with several relevant previous studies.

Ref	Freq (GHz)	Substrate material	Gain (dB)	Proposed technique	Area (mm ²)/ λ	Applications	Design complexity
[20]	3.5	FR-4	6.04	Complementary split-ring resonator (CSRR)	35 × 40/ 0.85 × 0.98	WLAN/WiMAX	Simple
[29]	2.4	Rogers RO3003C	5.1	Artificial magnetic conductor (AMC)	130.8 × 130.8/ 2.64 × 2.64	Indoor/outdoor wireless body area network (WBAN)	Simple
[30]	10	FR-4	2 to 5.8	Split-ring resonator (SRR)	48 × 35/ 1.17 × 0.85	5G	Complex
[32]	4.3	Rogers RT/Duroid 5880	4.85	Defected ground plane (DGS)	58 × 22/1 × 0.38	GPS	Simple
[33]	0.9 to 2.6	FR-4	2.6–4.6	Stepped cut at four corners	51 × 40/ 1.25 × 0.98	LTE	Simple
[34]	2.45, 3.5, 4.6, 5.8	FR-4	4.93, 5.92, 5.54, 4.95	Artificial magnetic conductor (AMC)	50 × 50/ 1.22 × 1.22	WLAN, WiMAX, and 5G	Complex
This work	3.5	Rogers RT/Duroid 5880LZ	6.0	Artificial magnetic conductor (AMC)	40 × 30/ 0.69 × 0.51	5G	Simple

proposed AMC surface at the desired frequency band of 3.5 GHz is illustrated in Figure 8. It can be seen that the gain of the antenna before placing the AMC is relatively low. To achieve the higher gain with a compact size, the introduction of the AMC plane behind the antenna increased its gain up to 65% in comparison with the antenna without the AMC backing. A comparison between simulated and measured radiation patterns with and without AMC is shown in Figure 9. From the 2D radiation pattern, it can be observed that the proposed antenna has shown a quasi-omnidirectional radiation pattern without the AMC and became more directional when integrated with the AMC. This gain increase can be explained by the constructive phase introduced by the AMC plane from behind the antenna. Another important consideration to ensure effective gain improvement is the spacing between the antenna and the AMC surface.

The antenna was measured in terms of reflection coefficient (S_{11}) using a vector network analyzer (VNA) (Agilent

8722ES), as shown in Figure 10. On the other hand, its radiation patterns were measured in an anechoic chamber room, as shown in Figure 11. Table 3 compares the proposed planar monopole antenna with previous studies. From the comparison table, it can be seen that the proposed design is relatively compact in size and higher in gain. As shown in Figure 10, the peak gain of the antenna is compared with and without the AMC backing. The peak gain of the AMC-backed antenna is improved to 6.08 dB at 3.5 GHz. The gain without an AMC antenna is 2.8 dB at 3.5 GHz.

6. Conclusion

In this paper, we use MTM in an inspired planar monopole antenna backed by an AMC plane is proposed in this work. The design process of the planar monopole antenna, AMC unit cell, and AMC plane has been presented, with the proposal of an equivalent circuit model. Simulations

indicated that the operating range frequency of the planar monopole antenna with and without MTM is from 3.3 to 3.5 GHz and 3.41 to 3.67 GHz, respectively. On the other hand, the measurements indicated good agreements with simulations, with an operation between 3.4 and 3.6 GHz for 5G application. Due to the AMC backing, the monopole antenna also showed improved reflection coefficient and gain improvements, from 2.7 dB (without AMC) to 6 dB at 3.5 GHz, while maintaining a compact size. This indicates the potential of the proposed AMC-backed antenna for 5G application.

Data Availability

Data sharing is not applicable to this article as no new data were created or analyzed in this study.

Conflicts of Interest

The authors declare that they have no conflicts of interest.

Acknowledgments

This work was supported in part by the Kementerian Pengajian Tinggi (KPT), and in part by Universiti Teknologi Malaysia under the research Grant, Q.J130000.21A2.05E25, 4B536, 01M98, 4B536 and 01M98.

References

- [1] S. Martin-Anton and D. Segovia-Vargas, "Fully planar dual-polarized broadband Antenna for 3G, 4G and sub 6-GHz 5G base stations," *IEEE Access*, vol. 8, Article ID 91940, 2020.
- [2] S. A. Ali Abdulateef Abdulbari, M. Mohammed Jawad, H. O. Hanoosh, M. Ali Saare, S. A. Lashari, and S. Ali Sari, "Design compact microstrap patch antenna with T-shaped 5G application," *Bull. Electr. Eng. Informatics*, vol. 10, no. 4, pp. 2072–2078, 2021.
- [3] M. Alibakhshikenari, B. S. Virdee, L. Naser-Moghadasi et al., "A comprehensive survey of "metamaterial transmission-line based antennas: design, challenges, and applications,"" *IEEE Access*, vol. 8, Article ID 144778, 2020.
- [4] M. Alibakhshikenari, B. S. Virdee, C. H. See, R. A. Abd-Alhameed, F. Falcone, and E. Limiti, "Surface wave reduction in antenna arrays using metasurface inclusion for MIMO and SAR systems," *Radio Science*, vol. 54, no. 11, pp. 1067–1075, 2019.
- [5] M. Ciydem and E. A. Miran, "Dual-polarization wideband sub-6 GHz suspended patch antenna for 5G base station," *IEEE Antennas and Wireless Propagation Letters*, vol. 19, no. 7, pp. 1142–1146, 2020.
- [6] A. Schumacher, R. Merz, and A. Burg, "3.5 GHz coverage assessment with a 5G testbed," in *Proceedings of the 2019 IEEE 89th veh Technol Conf*, pp. 1–6, Kuala Lumpur, Malaysia, May 2019.
- [7] M. Alibakhshikenari, B. S. Virdee, P. Shukla et al., "Metamaterial-inspired antenna array for application in microwave breast imaging systems for tumor detection," *IEEE Access*, vol. 8, Article ID 174667, 2020.
- [8] R. Bansal and N. Haven, "Antenna theory; analysis and design," *Proceedings of the IEEE*, vol. 72, no. 7, pp. 989–990, 1984.
- [9] O. Borazjani, M. Naser-Moghadasi, J. Rashed-Mohassel, and R. Sadeghzadeh, "Design and fabrication of a new high gain multilayer negative refractive index metamaterial antenna for X-band applications," *International Journal of RF and Microwave Computer-Aided Engineering*, vol. 30, no. 9, pp. 1–12, 2020.
- [10] D. Dan Sun, W. Wenbin Dou, L. Lizhi You, X. Xuequan Yan, and R. Rong Shen, "A broadband proximity-coupled stacked microstrip antenna with cavity-backed configuration," *IEEE Antennas and Wireless Propagation Letters*, vol. 10, pp. 1055–1058, 2011.
- [11] W. W. Li, C. Wang, Y.-Q. Lai, and J.-H. Zhou, "A compact dual-polarized cavity-backed annular slot antenna for indoor mimo systems," *Microwave and Optical Technology Letters*, vol. 57, no. 2, pp. 384–388, 2015.
- [12] A. M. Hamzah, L. Audah, N. Alkhafaji, H. J. Mohammed, and A. Abdulateef Abdulbari, "Substrate integrated waveguide SIW technology-based miniaturization and performance enhancement of antennas," *Int. J. Adv. Sci. Technol.* vol. 29, no. 6, pp. 1739–1754, 2020.
- [13] A. Dastranj, "Very small planar broadband monopole antenna with hybrid trapezoidal-elliptical radiator," *IET Microwaves, Antennas & Propagation*, vol. 11, no. 4, pp. 542–547, 2017.
- [14] J. Ju, "A novel compact UWB monopole antenna with enhanced bandwidth using triangular defected microstrip structure and stepped cut technique," *Microwave and Optical Technology Letters*, vol. 58, no. 6, pp. 1561–1563, 2016.
- [15] J. K. Pakkathillam and M. Kanagasabai, "Circularly polarized broadband Antenna deploying fractal slot geometry," *IEEE Antennas and Wireless Propagation Letters*, vol. 14, pp. 1–4, 2015.
- [16] M. Alibakhshi-Kenari, M. Naser-Moghadasi, R. Ali Sadeghzadeh, B. Singh Virdee, and E. Limiti, "New Compact antenna based on simplified CRLH-TL for UWB wireless communication systems," *International Journal of RF and Microwave Computer-Aided Engineering*, vol. 26, no. 3, pp. 217–225, 2016.
- [17] H. Hu, F. Chen, Q. Chu, and S. Member, "A wideband U-shaped slot antenna and its application in MIMO terminals," *IEEE Antennas and Wireless Propagation Letters*, vol. 15, pp. 1–4, 2015.
- [18] T. A. Elwi and A. M. Al-Saegh, "Further realization of a flexible metamaterial-based antenna on indium nickel oxide polymerized palm fiber substrates for RF energy harvesting," *International Journal of Microwave and Wireless Technologies*, vol. 13, no. 1, pp. 67–75, 2021.
- [19] A. A. Abdulbari, Z. Zakaria, S. K. Abdul Rahim, Y. M. Hussein, M. M. Jawad, and A. M. Hamzah, "Design and development broadband monopole antenna for in-door application," *TELKOMNIKA (Telecommunication Computing Electronics and Control)*, vol. 18, no. 1, p. 51, 2020.
- [20] G. Geetharamani and T. Aathmanesan, "A metamaterial inspired tapered patch antenna for WLAN/WiMAX applications," *Wireless Personal Communications*, vol. 113, no. 2, pp. 1331–1343, 2020.
- [21] C. Soemphol and N. Angkawisittpan, "Coplanar waveguide-fed ultra-wideband antenna with WLAN band," *Indonesian Journal of Electrical Engineering and Computer Science*, vol. 21, no. 3, p. 1523, 2021.
- [22] A. A. Abdulbari, S. K. Abdul Rahim, P. J. Soh, M. H. Dahri, A. A. Eteng, and M. Y. Zeain, "A review of hybrid couplers: state-of-the-art , applications, design issues and challenges," *International Journal of Numerical Modelling: Electronic Networks, Devices and Fields*, vol. 34, no. 5, pp. 1–19, 2021.

- [23] T. A. Elwi, "Remotely controlled reconfigurable antenna for modern 5G networks applications," *Microwave and Optical Technology Letters*, vol. 63, no. 8, pp. 2018–2023, 2021.
- [24] T. A. Elwi, Z. A. Abdul Hassain, and O. A. Tawfeeq, "Hilbert metamaterial printed antenna based on organic substrates for energy harvesting," *IET Microwaves, Antennas & Propagation*, vol. 13, no. 12, pp. 2185–2192, 2019.
- [25] M. Alibakhshikenari, B. S. Virdee, A. A. Althuwayb et al., "Study on on-chip antenna design based on metamaterial-inspired and substrate-integrated waveguide properties for millimetre-wave and THz integrated-circuit applications," *Journal of Infrared, Millimeter and Terahertz Waves*, vol. 42, no. 1, pp. 17–28, 2021.
- [26] A. Bakhtiari, R. A. Sadeghzadeh, and M. N. Moghadasi, "Gain enhanced miniaturized microstrip patch antenna using metamaterial superstrates," *IETE Journal of Research*, vol. 65, no. 5, pp. 635–640, 2019.
- [27] K. Suvarna, N. Ramamurthy, and D. V. Vardhan, "Miniaturized and gain enhancement of tapered patch antenna using defected ground structure and metamaterial superstrate for gps applications," *Progress In Electromagnetics Research C*, vol. 108, pp. 187–200, 2021.
- [28] Q. Liu, H. Liu, W. He, and S. He, "A low-profile dual-band dual-polarized antenna with an AMC reflector for 5G communications," *IEEE Access*, vol. 8, Article ID 24072, 2020.
- [29] Y. Gong, S. Yang, B. Li, Y. Chen, F. Tong, and C. Yu, "Multi-band and high gain antenna using AMC ground characterized with four zero-phases of reflection coefficient," *IEEE Access*, vol. 8, Article ID 171457, 2020.
- [30] K. N. Paracha, S. K. A. Rahim, P. J. Soh et al., "A low profile, dual-band, dual polarized antenna for indoor/outdoor wearable application," *IEEE Access*, vol. 7, no. c, Article ID 33277, 2019.
- [31] H. Sakli, C. Abdelhamid, C. Essid, and N. Sakli, "Metamaterial-based antenna performance enhancement for MIMO system Applications," *IEEE Access*, vol. 9, no. 4, Article ID 38546, 2021.
- [32] J. D. Baena, J. Bonache, F. Martin et al., "Equivalent-circuit models for split-ring resonators and complementary splitting resonators coupled to planar transmission lines," *IEEE Transactions on Microwave Theory and Techniques*, vol. 53, no. 4, pp. 1451–1461, 2005.
- [33] N. Ortiz, F. Falcone, and M. Sorolla, "Gain improvement of dual band Antenna based on complementary rectangular split-ring resonator," *ISRN Communications and Networking*, vol. 2012, Article ID 951290, 9 pages, 2012.
- [34] A. Moradikordalivand, T. A. Rahman, S. Ebrahimi, and S. Hakimi, "An equivalent circuit model for broadband modified rectangular microstrip-fed monopole antenna," *Wireless Personal Communications*, vol. 77, no. 2, pp. 1363–1375, 2014.